Assessing adaptive optics for fast polarization switching of synchrotron light for X-ray magnetic circular dichroism

Johnny Ho^a, Antoine Islegen-Wojdyla^a, Xiaoya Chong^a, Ali Sabbah^a, Kenneth A. Goldberg^a, and Alpha T. N'Diaye^a

^aLawrence Berkeley National Laboratory, 1 Cyclotron Road, Berkeley, CA 94720, USA

ABSTRACT

X-ray magnetic circular dichroism (XMCD), an experimental technique that utilizes circularly polarized light at synchrotron light sources to probe the magnetic properties of materials, is performed by taking the difference of two X-ray absorption spectroscopy (XAS) spectra with X-rays of opposite circular polarizations. Each XAS spectrum measurement requires an energy scan by rotating a diffraction grating, which takes on the order of minutes to complete. Variations in the light source beam conditions or sample material environment can occur in the time between each XAS measurement and can lead to systematic shifts and fluctuations in the collected spectra and ultimately affect the XMCD measurement. We describe a concept using adaptive optics with active feedback to enable the use of fast polarization switching with lock-in amplification to reduce these effects and increase the sensitivity of XMCD measurements, and the development of such an adaptive optics system at the Advanced Light Source that consists of a Hettrick-Underwood monochromator with a deformable pre-mirror, a variable-line-spacing planar grating, and a photon energy sensor at the exit slit for feedback control.

Keywords: XMCD, adaptive optics

1. INTRODUCTION

X-ray magnetic circular dichroism (XMCD) is an experimental technique that utilizes circularly polarized light at synchrotron light sources to probe the magnetic properties of materials. It is performed by taking the difference of two X-ray absorption spectroscopy (XAS) spectra with X-rays of opposite circular polarizations (Fig. 1).^{1–5} Each XAS spectrum measurement requires an energy scan by rotating a diffraction grating, which takes on the order of minutes to complete. Variations in the light source beam conditions or sample material environment can occur in the time between each XAS measurement, leading to systematic shifts and fluctuations in the collected spectra and ultimately affecting the XMCD measurement. Fast polarization switching (Fig. 2) and lock-in measurements have been suggested to improve XMCD measurements. Polarization switching has previously been implemented at synchrotron light sources, however, the implementation is slow or requires tuning the electron beam trajectory.^{6,7} A common challenge of this approach is maintaining the relative photon energy calibration and resolution between the two opposite polarizations of X-rays as they travel along different paths through the beam line. Here, we describe a concept using adaptive optics with active feedback to enable the use of fast polarization switching with lock-in amplification while maintaining a stable photon energy calibration.

2. ADAPTIVE OPTICS FOR XMCD

2.1 Energy shifts from spherical aberrations

Beamline 6.3.1, one of several beam lines used for XMCD spectroscopy at the Advanced Light Source (ALS), is a bending magnet beam line that consists of several refocusing mirrors and a Hettrick-Underwood monochromator (Fig. 3). Monochromatic X-rays that pass through the Beamline 6.3.1 monochromator should ideally be focused to the same vertical position at the exit slit plane (Fig. 4a); however, spherical aberrations from the pre-mirror

Further author information:

J.H.: E-mail: johnnyho@lbl.gov

A.I.W.: E-mail: awojdyla@lbl.gov, Telephone: +1 (510) 486-6153 A.T.N.: Email: atndiaye@lbl.gov, Telephone: +1 (510) 486-5926

(M2) of the monochromator will cause the X-rays to be unfocused at the exit slit plane (Fig. 4b) leading to energy shifts. These energy shifts can be experimentally measured by moving the aperture vertically and taking an X-ray absorption spectrum measurement for each aperture position; such an aperture scan is shown in Fig. 5 for the Co L₃ edge where the energy shifts are on the order of a few eV. Furthermore, energy shifts have been shown to vary with the shape of M2 by introducing bends to the upstream and downstream ends of M2 (Fig. 6). Fig. 5 also shows an example of where the aperture position might typically be set for linear, right-handed circular, and left-handed circular polarizations. Different energy calibrations must be applied for each polarization due to the energy shifts, making fast polarization switching a challenge. We propose a project called Monoplus to use a Hettrick-Underwood monochromator with a deformable pre-mirror and a novel photon energy sensor to monitor the photon energy at the exit slit plane in an active feedback loop to mitigate these energy shifts while maintaining a stable photon energy calibration.

2.2 Optimization of a deformable mirror to minimize energy shifts

The simulation software packages* shadow38 and xrt9 were used to model Beamline 6.3.1 for ray tracing (Fig. 7) to produce simulated energy shifts. Simulated energy shifts are shown for a spherical M2 with no bends in Fig. 8a and a spherical M2 with "realistic" bends in Fig. 8b using monochromatic beams of 840 eV to 900 eV (in steps of 10 eV) as the photon source.

In order to determine the shape of a deformable pre-mirror that would minimize energy shifts, we perform the following procedure for a ray tracing result with a monochromatic beam as the photon source. For the j^{th} aperture position, we compute the mean vertical position of the M_j photons at the exit slit plane

$$\bar{z}_j = \frac{1}{M_j} \sum_{k}^{M_j} z_k,\tag{1}$$

which characterizes the energy shift, and the root mean square deviation (RMSD)

$$RMSD_j = \sqrt{\frac{1}{M_j} \sum_{k}^{M_j} (z_k - \bar{z}_j)^2},$$
(2)

which characterizes the energy resolution. We then construct the following cost function for minimization

$$\sum_{j}^{N} (|\bar{z}_{j}| + \text{RMSD}_{j}) \tag{3}$$

where N is the total number of aperture positions. The result of our optimization is shown in Fig. 9 where the energy shifts have been mitigated.

2.3 Photon energy sensor

To monitor X-ray energies, a novel photon energy sensor consisting of a complementary metal—oxide—semiconductor (CMOS) image sensor with a cerium-doped yttrium aluminum garnet (YAG:Ce) scintillator window will be mounted on the upstream side of the exit slit plane as shown in Fig. 10a. The YAG:Ce scintillator will be coated with different thin metal films (Ti, Mn, Fe, Co, Ni, Cu, and Gd) with distinct absorption edges, resulting in reductions in photon intensity observed at various vertical positions on the CMOS image sensor (Fig. 10b).

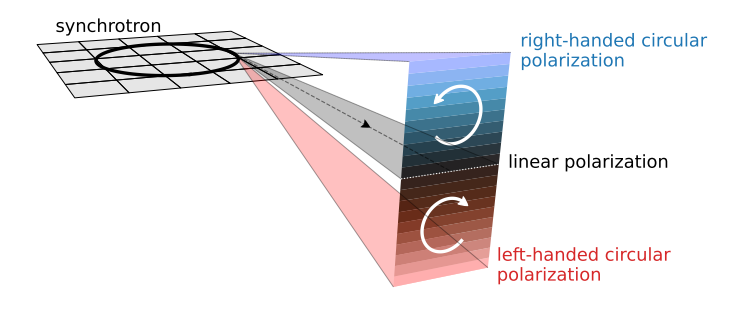
3. SUMMARY

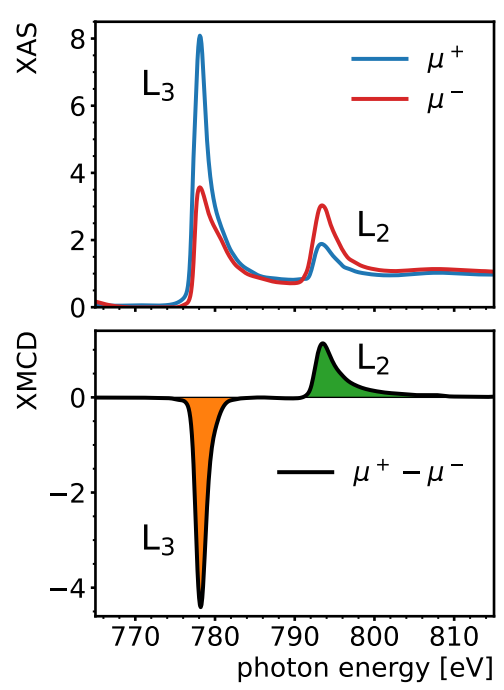
We have demonstrated with our simulation studies that we can fine tune energy shifts with a deformable premirror in a Hettrick-Underwood monochromator. We are currently developing a novel photon energy sensor that will be used together with a deformable mirror in a closed feedback loop for an adaptive optics system which will be implemented and demonstrated at Beamline 6.3.1 of the ALS. This adaptive optics system will enable us to perform fast polarization switching while maintaining stable photon energy calibrations to produce fast, high-precision XMCD measurements.

^{*}We use both shadow3 and xrt to cross-check that our simulation results are consistent.

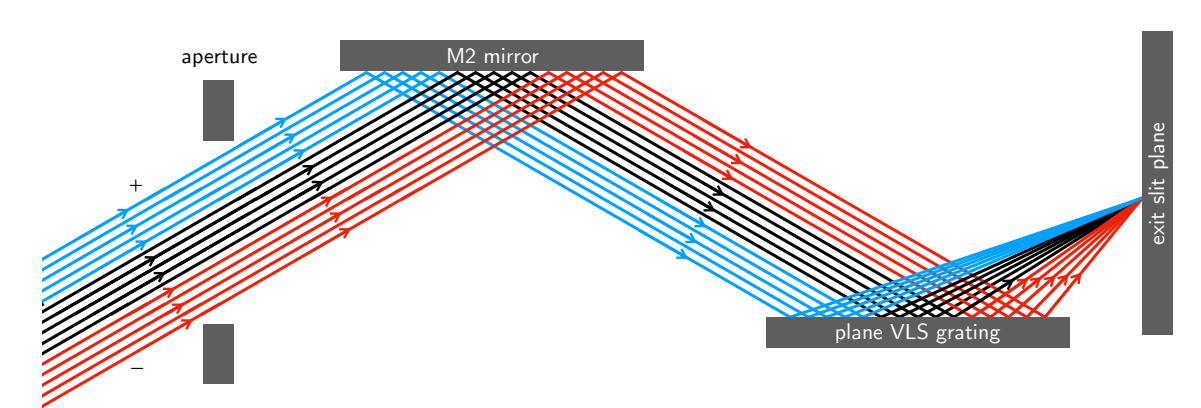
REFERENCES

- [1] Chen, C. T., Idzerda, Y. U., Lin, H.-J., Smith, N. V., Meigs, G., Chaban, E., Ho, G. H., Pellegrin, E., and Sette, F., "Experimental Confirmation of the X-Ray Magnetic Circular Dichroism Sum Rules for Iron and Cobalt," Phys. Rev. Lett. 75, 152–155 (July 1995).
- [2] Nakajima, R., Stöhr, J., and Idzerda, Y. U., "Electron-yield saturation effects in L-edge x-ray magnetic circular dichroism spectra of Fe, Co, and Ni," *Phys. Rev. B* **59**, 6421–6429 (March 1999).
- [3] Stöhr, J. and Siegmann, H., [Magnetism: From Fundamentals to Nanoscale Dynamics], Springer Series in Solid-State Sciences, Springer Berlin Heidelberg (2006).
- [4] van der Laan, G. and Figueroa, A. I., "X-ray magnetic circular dichroism—A versatile tool to study magnetism," Coord. Chem. Rev. 277–278, 95–129 (October 2014). Following Chemical Structures using Synchrotron Radiation.
- [5] Vaz, C. A. F., van der Laan, G., Cavill, S. A., Dürr, H. A., Rodríguez, A. F., Kronast, F., Kuch, W., Sainctavit, P., Schütz, G., Wende, H., Weschke, E., and Wilhelm, F., "X-ray magnetic circular dichroism," Nat. Rev. Methods Primers 5 (May 2025).
- [6] Sirotti, F., Polack, F., Cantin, J. L., Sacchi, M., Delaunay, R., Meyer, M., and Liberati, M., "SB7: the new bending-magnet double-headed dragon beamline at SuperACO," J. Synchrotron Radiat. 7, 5–11 (January 2000).
- [7] Holldack, K., Schüssler-Langeheine, C., Goslawski, P., Pontius, N., Kachel, T., Armborst, F., Ries, M., Schälicke, A., Scheer, M., Frentrup, W., and Bahrdt, J., "Flipping the helicity of X-rays from an undulator at unprecedented speed," *Commun. Phys.* 3 (April 2020).
- [8] Sanchez del Rio, M., Canestrari, N., Jiang, F., and Cerrina, F., "SHADOW3: a new version of the synchrotron X-ray optics modelling package," J. Synchrotron Radiat. 18, 708–716 (September 2011).
- [9] Klementiev, K. and Chernikov, R., "Powerful scriptable ray tracing package xrt," in [Advances in Computational Methods for X-Ray Optics III], del Rio, M. S. and Chubar, O., eds., 9209, 92090A, International Society for Optics and Photonics, SPIE (September 2014).
- [10] Nachimuthu, P., Underwood, J. H., Kemp, C. D., Gullikson, E. M., Lindle, D. W., Shuh, D. K., and Perera, R. C., "Performance Characteristics of Beamline 6.3.1 from 200 eV to 2000 eV at the Advanced Light Source," in [Synchrotron Radiation Instrumentation: Eighth International Conference on Synchrotron Radiation Instrumentation], Warwick, T., Arthur, J., Padmore, H. A., and Stöhr, J., eds., AIP Conf. Proc. 704, 454–457 (May 2004).



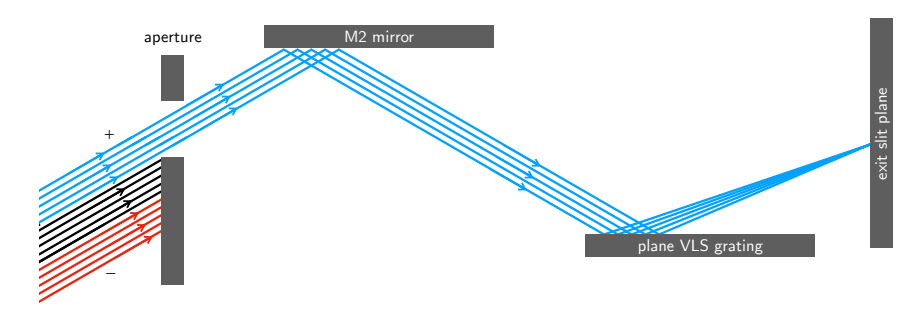


- (a) Diagram of synchrotron radiation from a bending magnet with linearly polarized light in the plane of the synchrotron ring, righthanded circularly polarized light above the plane, and left-handed circularly polarized light below the plane
- (b) X-ray absorption (top) and X-ray magnetic circular dichroism (bottom) spectra for the Co L_3 and L_2 edges (figure adapted from Ref. 4)

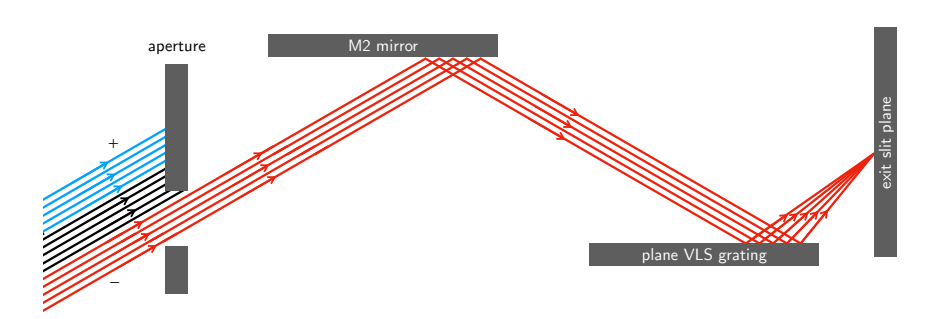


 $\begin{tabular}{l} (c) \ Diagram \ of \ X-rays \ of \ linear \ and \ circular \ polarizations \ passing \ through \ a \ variable-line-spacing \ (VLS) \ plane \ grating \ monochromator \end{tabular}$

Figure 1: X-ray magnetic circular dichroism is a technique used to study the magnetic properties of quantum materials by taking the difference between two X-ray absorption spectra of a sample material in a magnetic field: one spectrum taken with right-handed circularly polarized X-rays and another spectrum taken with left-handed circular polarized X-rays.



(a) Right-handed circularly polarized light passing through the aperture



(b) Left-handed circularly polarized light passing through the aperture

Figure 2: Fast polarization switching for XMCD at a bending magnet beam line involves alternating between right- and left-handed circularly polarized X-rays with a moving aperture. It requires X-rays of both polarizations to be focused upon the same vertical position on the exit slit plane.

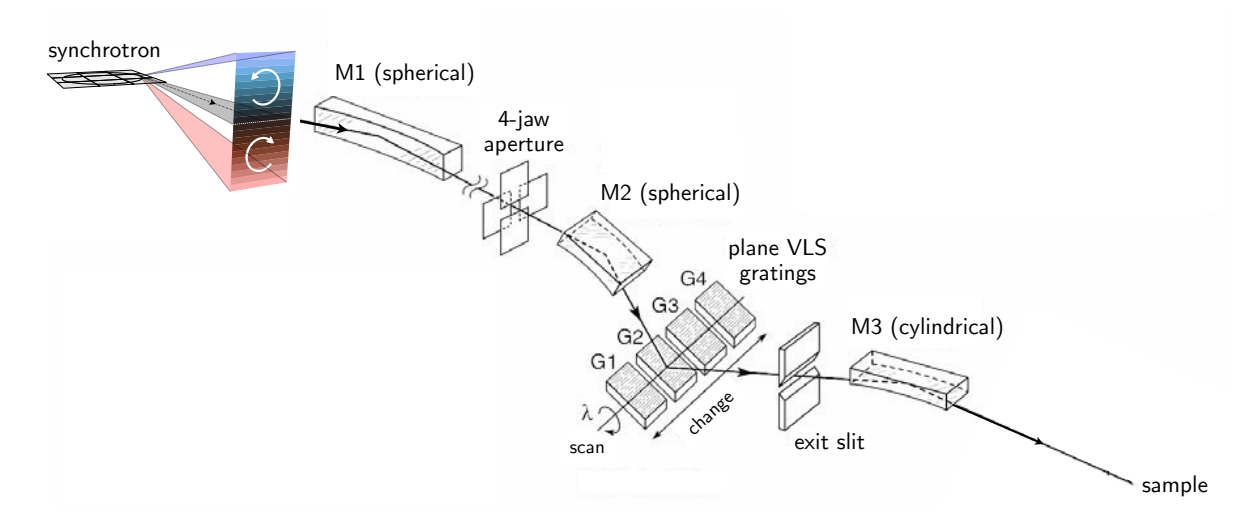
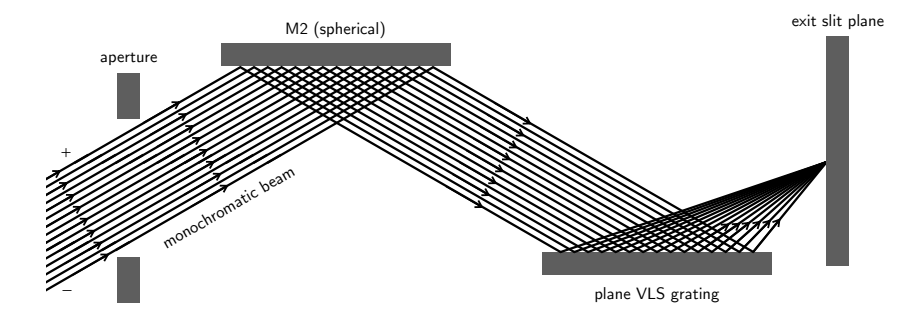
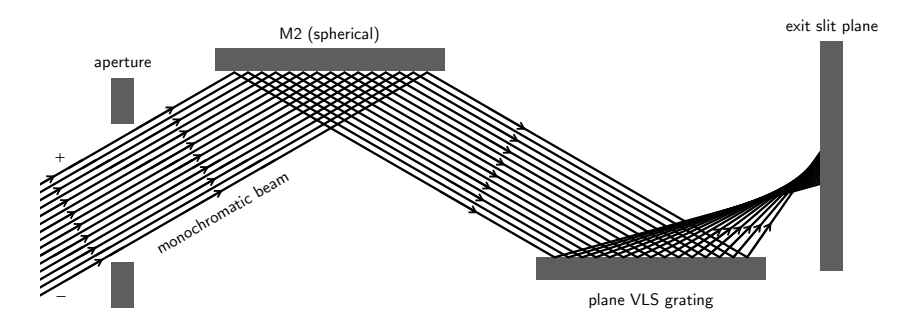


Figure 3: Diagram of Beamline 6.3.1, a bending magnet beam line that is primary used for X-ray magnetic circular dichroism spectroscopy at the Advanced Light Source (figure adapted from Ref. 10). The beam line optics consist of a horizontal focusing concave spherical mirror (M1), a 4-jaw aperture, a vertical focusing concave spherical mirror (M2), interchangeable planar VLS gratings, an exit slit, and a vertical focusing mirror (M3).



(a) Monochromatic beam passing through a grating monochromator without aberrations



(b) Monochromatic beam passing through a grating monochromator with aberrations

Figure 4: A monochromatic beam passing through a grating monochromator should be focused to the same vertical position on the exit slit plane (top). However, aberrations in the optical elements of the grating monochromator will cause the beam to be unfocused at the exit slit plane (bottom).

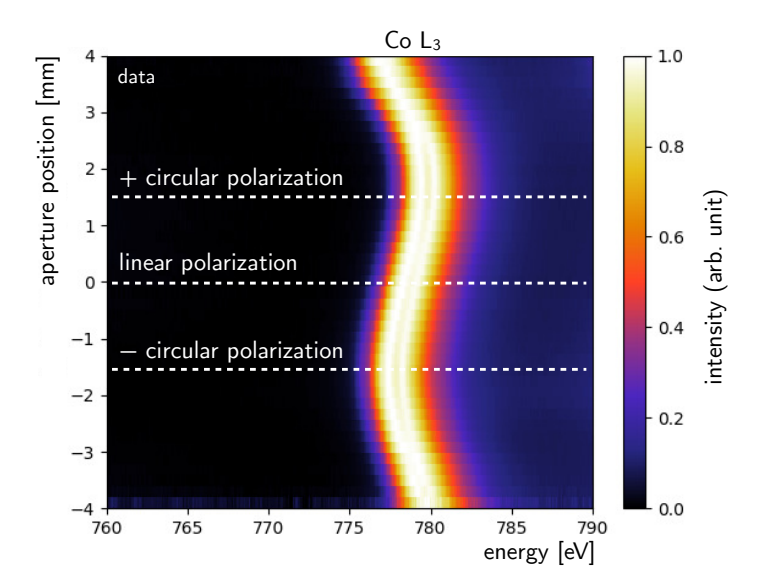


Figure 5: X-ray absorption spectra of the Co L_3 edge for various aperture positions at Beamline 6.3.1 where energy shifts on the order of a few eV are observed. Typical positions of the aperture for right-handed circular, linear, and left-handed circular polarizations are shown in horizontal dashed white lines.

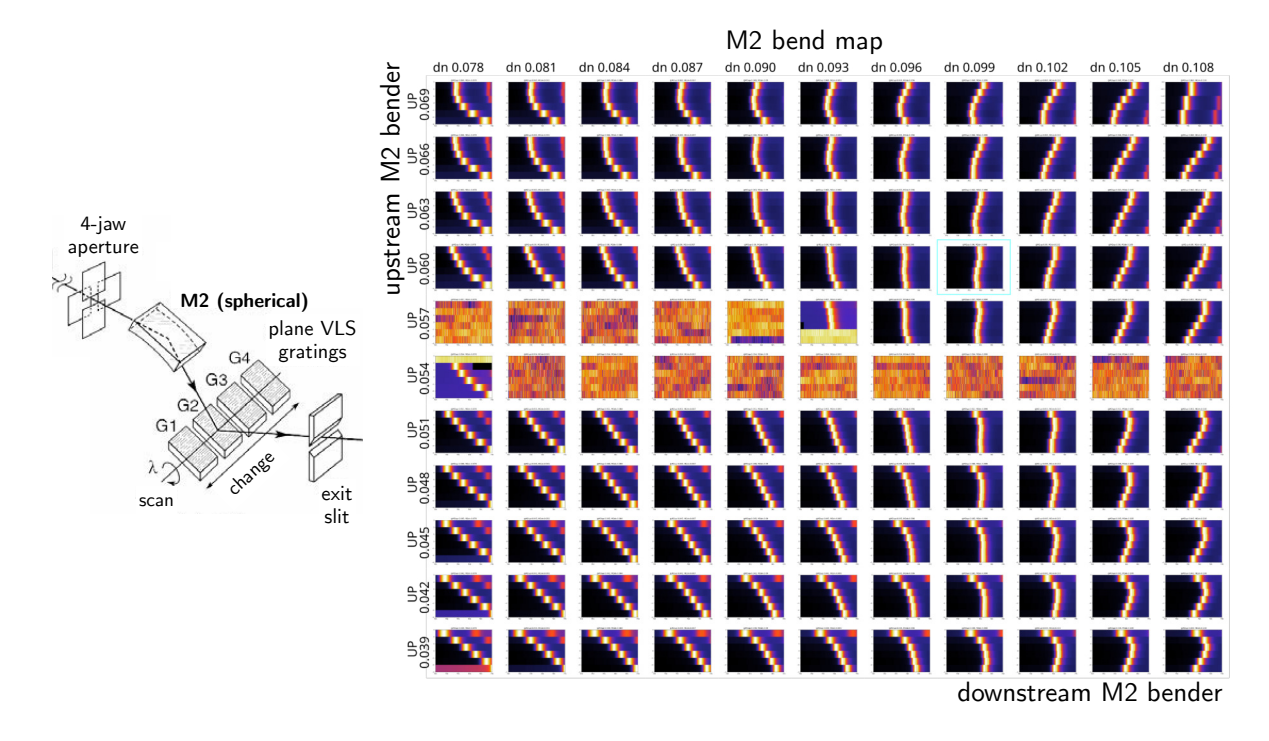


Figure 6: Aperture scans for different bend configurations of the monochromator pre-mirror (M2) at Beamline 6.3.1 demonstrating that the energy shifts vary with the shape of M2.

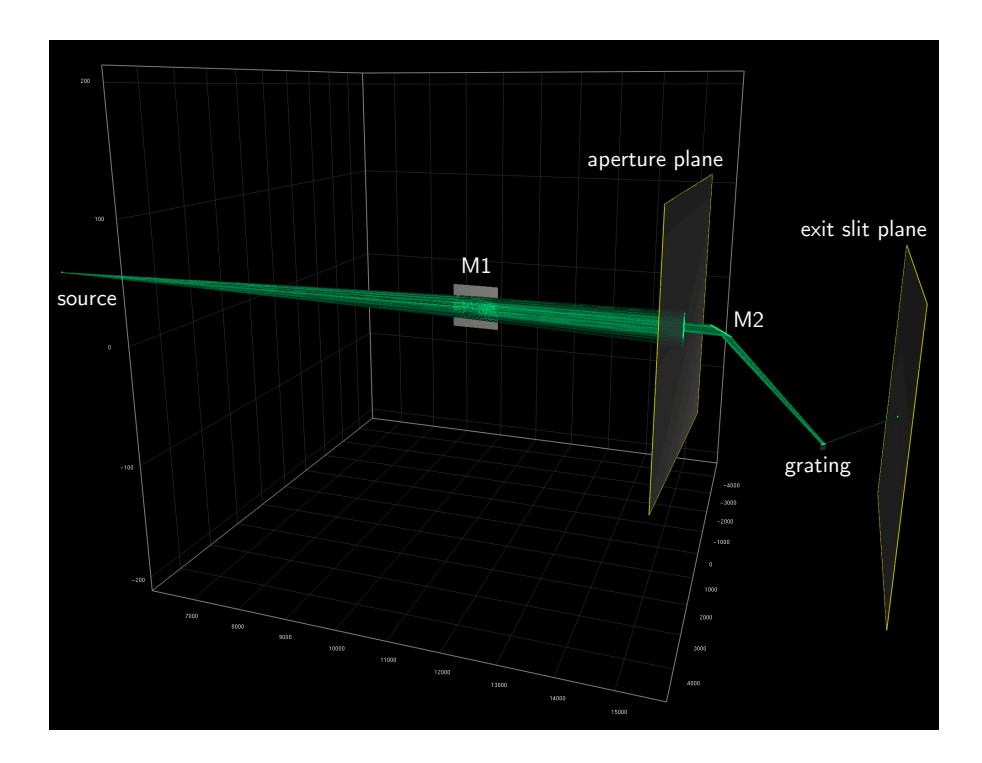
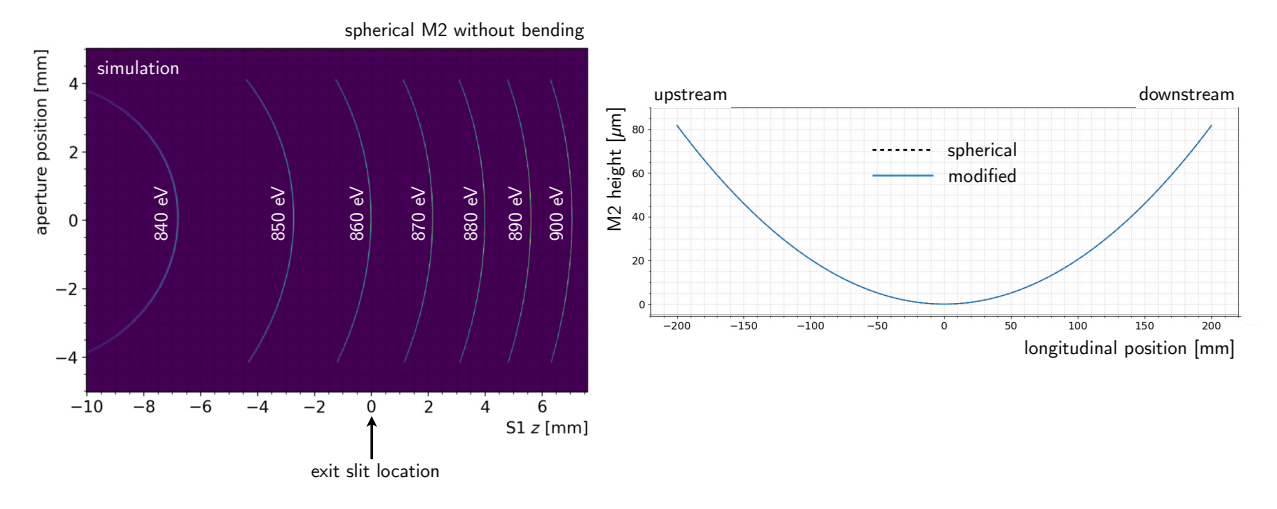
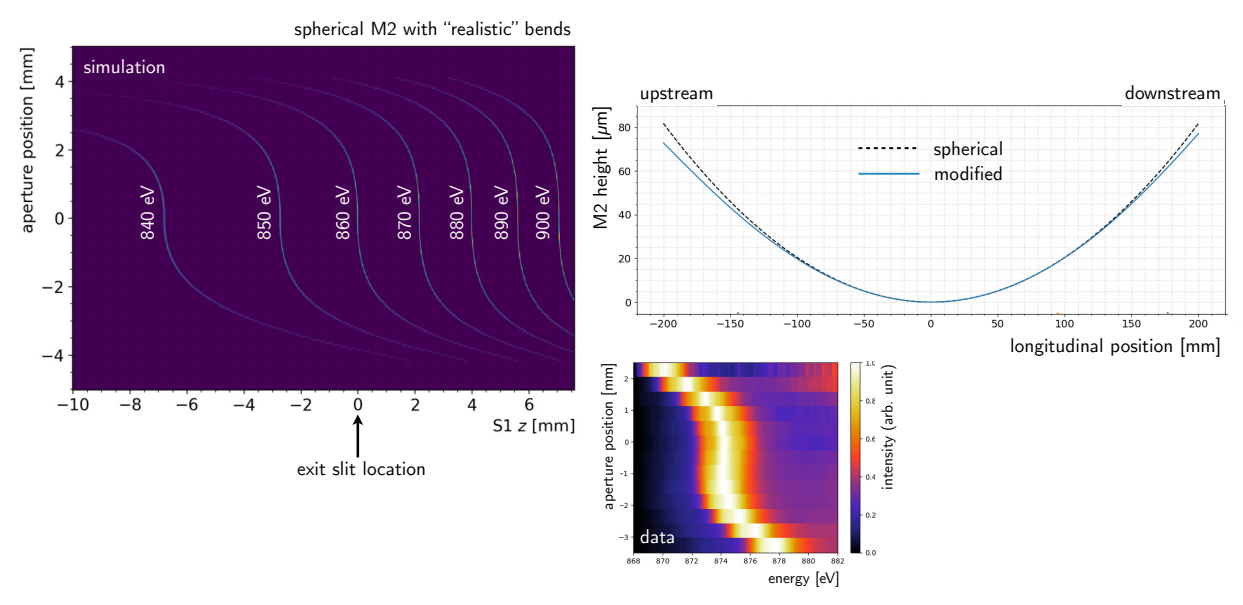


Figure 7: Ray tracing of Beamline 6.3.1 from the photon source to the exit slit plane with the xrt simulation software package (the aspect ratio is set such that the longitudinal axis appears much shorter than it actually is).



(a) Ray tracing simulation with a spherical M2 pre-mirror



(b) Ray tracing simulation with "realistic" bends on a spherical M2 pre-mirror

Figure 8: Simulated energy shifts for a spherical pre-mirror with no bends (top) and a spherical pre-mirror with realistic bends (bottom). The case with realistic bends resulted in simulated energy shifts that resembles energy shifts that are observed in our experimental data.

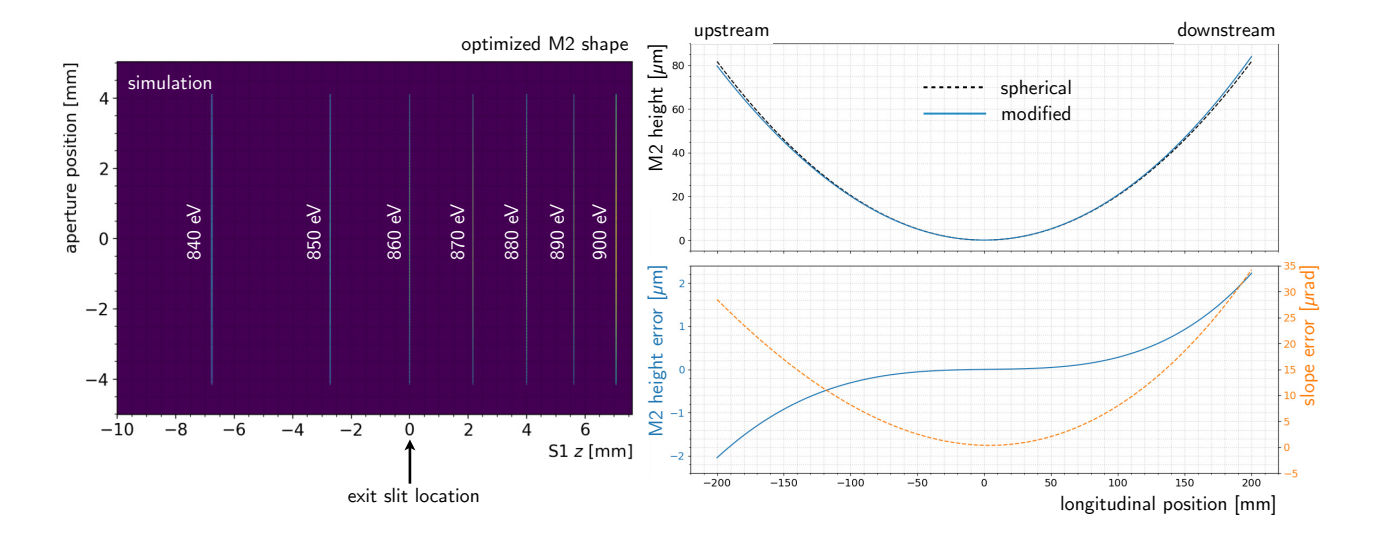
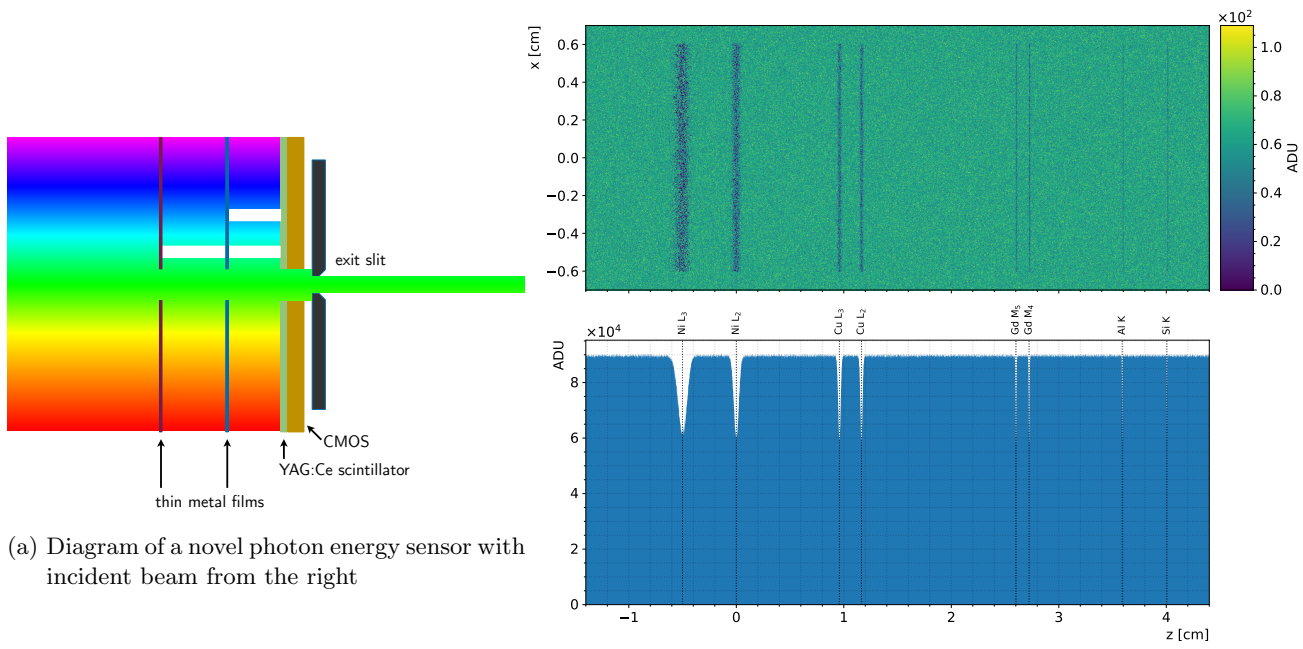


Figure 9: Simulated energy shifts with an optimized M2 pre-mirror shape.



(b) Toy simulation of the photon energy sensor where x corresponds to the horizontal position and z corresponds to the vertical position on the CMOS image sensor. The intensity reductions are modeled using Gaussian distributions with widths of 1 eV.

Figure 10: A novel photon energy sensor consisting of a CMOS image sensor with a YAG:Ce scintillator window coated with different thin metal films (top). The different thin metal films have absorption edges at distinct energies resulting in reduction of photon intensities at various vertical positions on the CMOS image sensor (bottom).